

Determination of the electric field intensity and space charge density versus height prior to triggered lightning

C. J. Biagi,¹ M. A. Uman,¹ J. Gopalakrishnan,² J. D. Hill,¹ V. A. Rakov,¹ T. Ngin,¹ and D. M. Jordan¹

Received 25 January 2010; revised 5 April 2011; accepted 19 April 2011; published 2 August 2011.

[1] We infer the vertical profiles of space charge density and electric field intensity above ground by comparing modeling and measurements of the ground-level electric field changes caused by elevating grounded lightning-triggering wires. The ground-level electric fields at distances of 60 m and 350 m were measured during six wire launches that resulted in triggered lightning. The wires were launched when ground-level electric fields ranged from 3.2 to 7.6 kV m^{-1} and the triggering heights ranged from 123 to 304 m. From wire launch time to lightning initiation time, the ground-level electric field reduction at 60 m ranged from 2.2 to 3.4 kV m^{-1} , with little ground-level electric field reduction being observed at 350 m. We observed that the triggering heights were inversely proportional to the ground-level electric field when the wires were launched. Our Poisson equation solver simulates the ground-level electric field changes as the grounded wires extend in assumed vertically varying profiles of space charge density and electric field intensity. Our model reproduces the measured ground-level electric field changes when the assumed space charge density decays exponentially with altitude, with ground-level charge densities between 1.5 and 7 nC m^{-3} , space charge exponential decay height constants ranging from 67 to 200 m, and uniform electric field intensities far above the space charge layer ranging from 20 to 60 kV m^{-1} . Our model predicts typical charge densities on the wires of some tens of $\mu\text{C m}^{-1}$ with milliampere-range currents flowing into the wires from ground to supply the wire charge.

Citation: Biagi, C. J., M. A. Uman, J. Gopalakrishnan, J. D. Hill, V. A. Rakov, T. Ngin, and D. M. Jordan (2011), Determination of the electric field intensity and space charge density versus height prior to triggered lightning, *J. Geophys. Res.*, 116, D15201, doi:10.1029/2011JD015710.

1. Introduction

1.1. Background

[2] The ambient electric field of thunderstorms causes electrical discharge known as corona from various types of sharp objects located on the ground, often creating a space charge layer near ground. The usually upward directed electric field due to negative cloud charges is reduced near ground by the presence of the positive corona space charge layer. A space charge layer (of either polarity) prevents the quasi-static (slowly varying over time scales of seconds to minutes) electric field at ground level from exceeding an absolute value of about 5 to 10 kV m^{-1} , while the field above the layer can be up to an order of magnitude higher [e.g., Standler and Winn, 1979; Chauzy and Raizonville, 1982; Soula and Chauzy, 1991; Willett et al., 1999]. When a sig-

nificant space charge layer is present near ground, the relatively large and fast field change from a lightning flash typically causes a polarity reversal at ground but not at altitude, and the field recovery following a large and fast field change occurs more rapidly at ground than aloft [e.g., Standler and Winn, 1979; Chauzy and Soula, 1987; Chauzy and Soula, 1989]. Thus, inferences of, for example, aspects of charge transfer and continuing current from electric field measurements at ground may be compromised by the presence of a space charge layer. Additionally, when attempting to artificially initiate (trigger) lightning using the rocket-and-wire technique [Rakov and Uman, 2003, chapter 7], the electric field at ground is used as an often inadequate proxy for the unknown triggering field at higher altitudes, and the variable field reduction of the space charge layer reduces the triggering efficiency. Although it would often be advantageous to measure the electric field above the space charge layer for the reasons given above, doing so presents logistical difficulties.

[3] Here we describe a novel method to infer the vertical profiles of atmospheric space charge density and the atmospheric electric field that does not require using elevated sensors. The method involves comparing measurements of the ground-level electric field change during the ascent of

¹Department of Electrical and Computer Engineering, University of Florida, Gainesville, Florida, USA.

²Department of Mathematics, University of Florida, Gainesville, Florida, USA.

a thin grounded wire, such as those used to trigger lightning, with corresponding predictions of numerical models. The present paper's organization is as follows: We review previous literature regarding the corona charge layer near ground and vertical atmospheric electric field profile. We describe our experiment and instrumentation, and we qualitatively describe the electric field changes that occur when a grounded wire is quickly extended upward below the thundercloud. Then, we present measurements of the ground-level electric field intensity versus time prior to initiation of the triggered-lightning upward positive leader (UPL) at distances of 60 m and 350 m for six triggered lightning flashes along with transient channel-base currents and field changes from impulsive charge deposition (precursors) ahead of the wire tip. We compare our measurements (accounting for field changes from precursor charge transfer) to numerical solutions of Poisson's equation for the electric field change everywhere in the computational domain as the wire is extended upward in assumed space charge layer with an assumed uniform electric field intensity far above this layer. We infer the induced charge on the wire as a function of wire height from the model-predicted radial component of electric field along the wire, and determine the current which must flow from ground to supply it. Finally, we relate our measurements of the prelaunch values of the ground-level electric field to those of other researchers. It should be noted that the data presented here were collected for the purposes of other experiments, and as such were not optimized for the experiment discussed herein. The method described here, when performed with optimally collected data, should prove even more valuable in determining the ambient electric field above ground, and thus increasing the triggering efficiency.

1.2. The Space Charge Layer due to Corona at Ground

[4] There are many reports of a significant space charge layer existing near the ground below thunderclouds. Thunderstorm electric fields have been found to have higher magnitudes over water, where a lack of sharp objects minimizes space charge production by corona current. *Toland and Vonnegut* [1977] reported a maximum electric field intensity of 130 kV m^{-1} over water (a lake). *Chauzy and Soula* [1989] simultaneously measured the electric field on the shore of a lagoon and on a raft that was 100 m away from land, and found that the electric field magnitude over the water was generally higher than over land.

[5] Several researchers have consistently reported measuring higher-magnitude electric fields above ground using field mills carried by balloon or rocket. In experiments at the Kennedy Space Center (KSC) in Florida and Langmuir Laboratory in New Mexico, *Standler and Winn* [1979] raised and lowered a field mill on a balloon between altitudes of 3 and 120 m altitude every few minutes to measure the electric field as a function of height while simultaneously measuring the ground-level electric field. They reported that when the ground level field exceeded 3 kV m^{-1} and 5 kV m^{-1} at KSC and Langmuir, respectively, the field aloft increased with altitude to a maximum of about 20 kV m^{-1} . They inferred a maximum charge density of 0.8 nC m^{-3} at a height between 30 and 50 m above ground, above which the charge density decreased. It is worth noting that *Standler and Winn* [1979] also reported measuring corona current flowing from "small evergreen trees" in New Mexico, and that the corona current

level rapidly increased when the ground-level electric field exceeded 5 kV m^{-1} . The maximum corona current from a tree measured by *Standler and Winn* [1979] was 600 nA in an electric field of 12 kV m^{-1} .

[6] In experiments in southwestern France, *Chauzy and Raizonville* [1982] reported five balloon-borne electric field soundings with simultaneous ground-level field measurements underneath thunderclouds. Three of the soundings were done with negative charge overhead and two with positive charge overhead. Their data showed that for both charge polarities overhead, the absolute value of electric field increased with altitude and became approximately constant at a height somewhere between 50 and 200 m above ground at levels between about 20 to 30 kV m^{-1} , while at the same time the absolute value of ground-level electric field remained constant and never exceeded about 5 kV m^{-1} . They inferred average space charge densities of 2 to 4 nC m^{-3} and space charge layer depths of about 100 to 200 m above ground when negative charge was overhead. When positive charge was overhead, they inferred a higher average space charge density of about -5 nC m^{-3} in a more shallow space charge layer that extended only up to a height of about 50 to 100 m above ground.

[7] In experiments in two different locations in France and in different years, *Chauzy and Soula* [1987], simultaneously measuring the electric field at ground and at a height of 15 m above ground, found that the field aloft was up to 10 kV m^{-1} greater than at ground level and an inferred charge density between about 3 and 6 nC m^{-3} .

[8] *Soula and Chauzy* [1991] simultaneously measured the electric field at ground and at four heights up to 803 m from an approaching storm at the KSC in Florida, during which there was no significant precipitation and four lightning flashes were triggered using the rocket-and-wire technique. The apparatus they used is described by *Chauzy et al.* [1991]. They found that ions created by corona at ground travel up to at least 600 m. They reported measuring a maximum electric field of 65 kV m^{-1} at an altitude of 603 m, while the ground-level field measured simultaneously did not exceed 5 kV m^{-1} . Their data indicated that the electric field became constant above 436 m. They inferred average space charge densities between the five electric field measurement heights that ranged from about 0.2 to 1 nC m^{-3} .

[9] *Chauzy and Soula* [1999], using the 'PICASSO' model [e.g., *Qie et al.*, 1994] with measurements made in Southern France, at KSC [*Soula and Chauzy*, 1991], and at the Camp Blanding Army National Guard Base, Florida [*Uman et al.*, 1996], examined the time evolution of corona space charge up to a height of 1 km within a $10 \text{ km} \times 10 \text{ km}$ area. *Chauzy and Soula* [1999] estimated that tens to a few hundreds of coulombs of corona space charge can be lifted to a height of 1 km via conduction or convection currents over periods of several tens of minutes, and thus the space charge may contribute to the development of the lower positive charge center in thunderclouds.

[10] *Willett et al.* [1999] probed the vertical electric field up to an altitude of about 4 km at Camp Blanding using field mills carried by a rocket that was launched roughly 5 seconds prior to the launch of a separate wire-extending rocket in 15 attempts to trigger lightning. They presented for two of their flights (flights 6 and 13 [*Willett et al.* [1999, Figures 14 and 18]) the electric field versus altitude soundings that

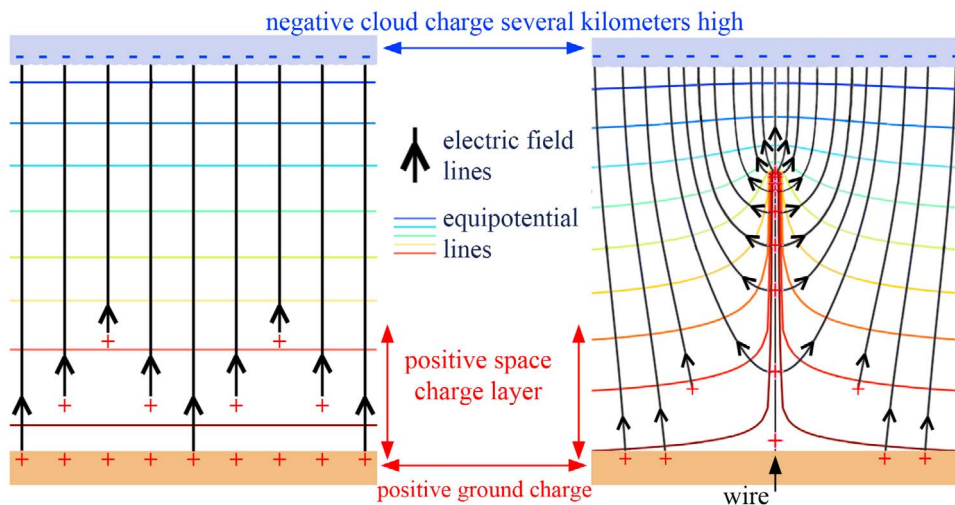


Figure 1. (left) An approximation of the electric field between negative thundercloud charge that is several kilometers above ground and ground surface. The vertical electric field, shown with black arrows, is a function of height in the space charge layer (red pluses). The horizontal equipotential lines (representing equipotential planes in 3-D space) are farther apart in the space charge layer than in the space-charge free region. (right) The electric field with the grounded triggering wire present.

showed that the electric field increased with altitude, an observation from which they inferred the presence of a space charge layer. In their flight 6 the ground-level electric field was about 7 kV m^{-1} , and it increased with height to about 15 kV m^{-1} at a height of about 60 m, above which the field stayed relatively constant. In flight 13 the ground-level electric field was about 6 kV m^{-1} , and it increased with height to about 24 kV m^{-1} at a height of about 500 m, above which the field stayed relatively constant. In both flights, the increasing electric field was attributed to space charge layers. For flight 13 they inferred an average space charge density of about 0.3 nC m^{-3} and noted that the charge density in the lower 60 m was probably three times this value. Willett *et al.* [1999] reported measuring a maximum electric field magnitude of 38 kV m^{-1} at altitudes between 3.2 and 3.7 km above ground.

2. Experiment

2.1. Instrumentation

[11] The observations described herein were made during the summers of 2009 and 2010 at the International Center for Lightning Research and Testing (ICLRT) at Camp Blanding in north central Florida, a facility that is operated jointly by the University of Florida and Florida Institute of Technology. Rockets trailing grounded triggering wires were launched from a 3 m tall launch tube apparatus on top of an 11 m high launch tower located near the center of the experimental site. The ICLRT occupies approximately 1 km^2 of land covered mostly by grasses and short shrubs, and is surrounded by dense pine woods with a canopy height of about 30 m. The ground at the ICLRT is relatively flat and does not have height variations of more than a few meters.

[12] The lightning-triggering wires were Kevlar-reinforced 0.2 mm diameter copper. In Launches 1 through 4 and 6, a straight and vertical conductor connected the launch tubes and triggering wire to a 25 m long ground rod. For Launch 5,

a 1 cm gap was placed in the vertical conductor connecting the launch tubes and ground (for the purposes of a separate experiment). The measured low-frequency, low-current grounding impedance was about 20Ω . Current above about 1 A in the triggering wire was measured at the launch tower using a noninductive shunt having a resistance of $1 \text{ m}\Omega$ from DC to 8 MHz, and a Pearson current transformer with a flat response over a frequency range 10 Hz to 5 MHz. Fast electric field changes (from precursors; see section 3.3) prior to the initiation of the sustained upward positive leader were measured using a capacitively coupled flat-plate sensor located 156 m north of the launch tower (henceforth referred to as 'E2'). The E2 sensor was designed to measure field intensities ranging from about 1 to 100 V m^{-1} and had a relaxation time constant (exponential decay time to a step function input) of about 10 ms. The flat-plate antenna was installed flush with ground, and because of its relatively high sensitivity, the sensor electronics saturated upon exposure to rain. A thin plastic dome was placed over the sensor to shield it from rain and prevent it from saturating, but doing so introduced uncertainty in the calibration of the sensor (further discussed in section 3.3 in relation to the comparison of precursor charges directly measured and inferred from E2). Both current measurements and the E2 measurement were bandwidth limited (low-pass filtered) to 3 MHz, and sampled at 10 MHz with 12-bit amplitude resolution.

[13] High-speed video images were recorded at a distance of 440 m from the launch tower with a Phantom V7.3 camera operating at framing rates between 5 and 10 kiloframes per second (kfps) with 14-bit gray scale resolution. The high-speed camera was equipped with either a 20 mm or a 24 mm focal-length lens providing a spatial resolution of 0.48 m or 0.40 m per pixel, respectively, and effective vertical fields of view for 800 pixels of 380 m and 320 m above ground level, respectively. The effective horizontal field of view was about 100 m centered on the

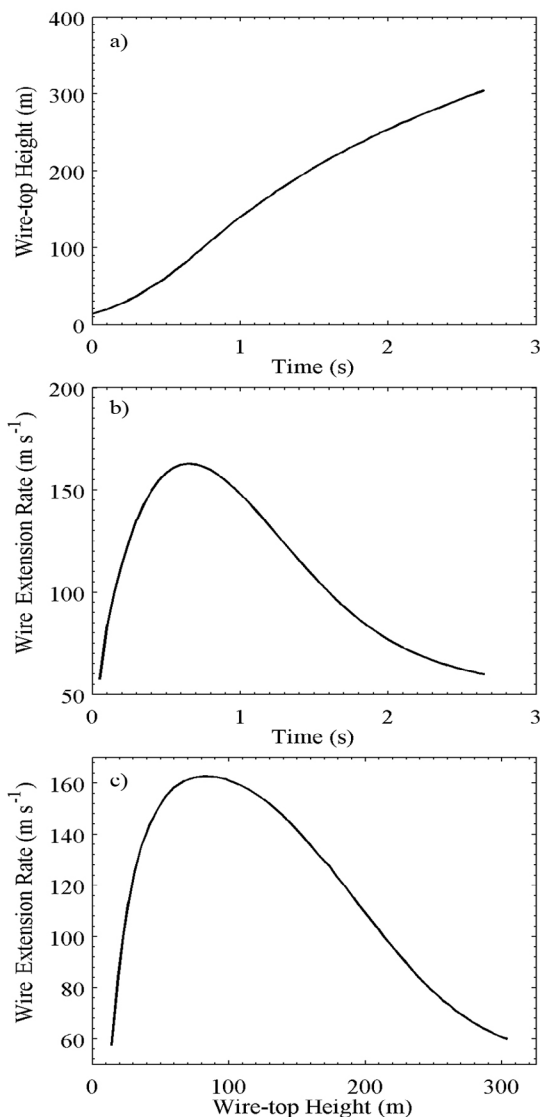


Figure 2. (a) The modeled wire-top height versus time, (b) the modeled wire extension rate versus time, and (c) the modeled wire extension rate versus the modeled wire-top height. The minimum wire height is the top of the launch tubes, or a height of 14 m.

launch tower. Each launch was also recorded in still images of 6 s exposure and high-definition (1080i) 30 fps video at various locations around the launch tower to provide a view of the wire from all directions. The high-speed video, wire-base currents, and fast electric field measurements were synchronized using GPS timing.

[14] The quasi-static electric field at ground level was recorded at distances of 60 m and 350 m to the northeast and northwest of the launch tower, respectively, with tripod-mounted Campbell Scientific CS110 field mills in the inverted configuration (sensor faces ground) sampling at 5 Hz, or every 200 ms. The field mills are specified by the manufacturer to have an accuracy of $\pm 5\%$. The amplitude resolution of the field mill measurements used here are limited to 100 V m^{-1} . The field mill data were recorded without GPS timing,

although an approximate time was supplied by the data storage computer that was sufficiently accurate (within a few seconds) to distinguish between different lightning flashes. The sampling for the two field mills was not synchronous. In this study, a positive electric field at ground corresponds to the field lines pointing upward (physics sign convention). Positive current and negative electric field change at ground correspond to the removal of negative charge from or the deposition of positive charge in the atmosphere.

2.2. The Wire Shielding Effect

[15] Figure 1 (left) illustrates the cloud charge, the space charge layer near ground, and the ground-surface charge assuming that (1) the cloud charge is uniformly distributed on an infinitely thin boundary at constant height of several kilometers with a horizontal extent that is much greater than its height above ground and (2) the space charge layer near ground is horizontally homogeneous. Under these approximations, the lines of equal potential (colored lines in Figure 1) are horizontally uniform. Correspondingly, the ambient electric field lines (the negative gradient of the potential, shown as solid black arrows) point vertically from the ground to the cloud (with no horizontal component), and the ambient electric field strength (represented by density of field lines) increases with increasing height in the space charge layer.

[16] Figure 1 (right) illustrates the ambient electric field profile when a thin and grounded conductor is quickly extended vertically from ground, as is done during the launch of a grounded wire to trigger lightning (this electric field profile is similar to that around a stationary tall object). As the wire ascends, an induced charge develops on the wire surface to cancel the tangential component of the ambient electric field on the surface of the conducting wire [Griffiths, 1981, chapter 2]. The line charge density on the wire surface is proportional to the radial field magnitude at the wire's surface according to Gauss's Law. The ground supplies the induced charge needed to keep the wire at ground potential. Corona from the wire pushes the induced charge radially outwards, creating a 'corona sheath' around the wire extending out several meters. In the modeling we will assume that the shielding effect at ground is the same if the charge is on the wire or in the corona sheath. The induced charge on the wire and in the corona sheath creates an electric field outside the wire that distorts the ambient electric field depicted in Figure 1 (left), forcing some of the ambient electric field lines that were vertical before the wire was launched to originate on the surface of the wire (or corona sheath) in the normal (radial) direction instead of originating on the ground. This results in a reduction of the electric field magnitude at ground near the wire.

[17] The induced charge per unit length on the wire (and surrounding electric field intensity) is highest at the top of the ascending wire. Eventually, current pulses at the wire tip (precursors) occur as the air undergoes significant dielectric breakdown [e.g., Lalande *et al.*, 1998; Willett *et al.*, 1999; Biagi *et al.*, 2009]. Each precursor deposits charge in the air (and delivers opposite charge to ground via current on the wire) that causes a field reduction at ground of the same polarity as the field reduction from the wire charges. As described in section 3.3, our measurements show that the charge of a single precursor is on average about $34 \mu\text{C}$,

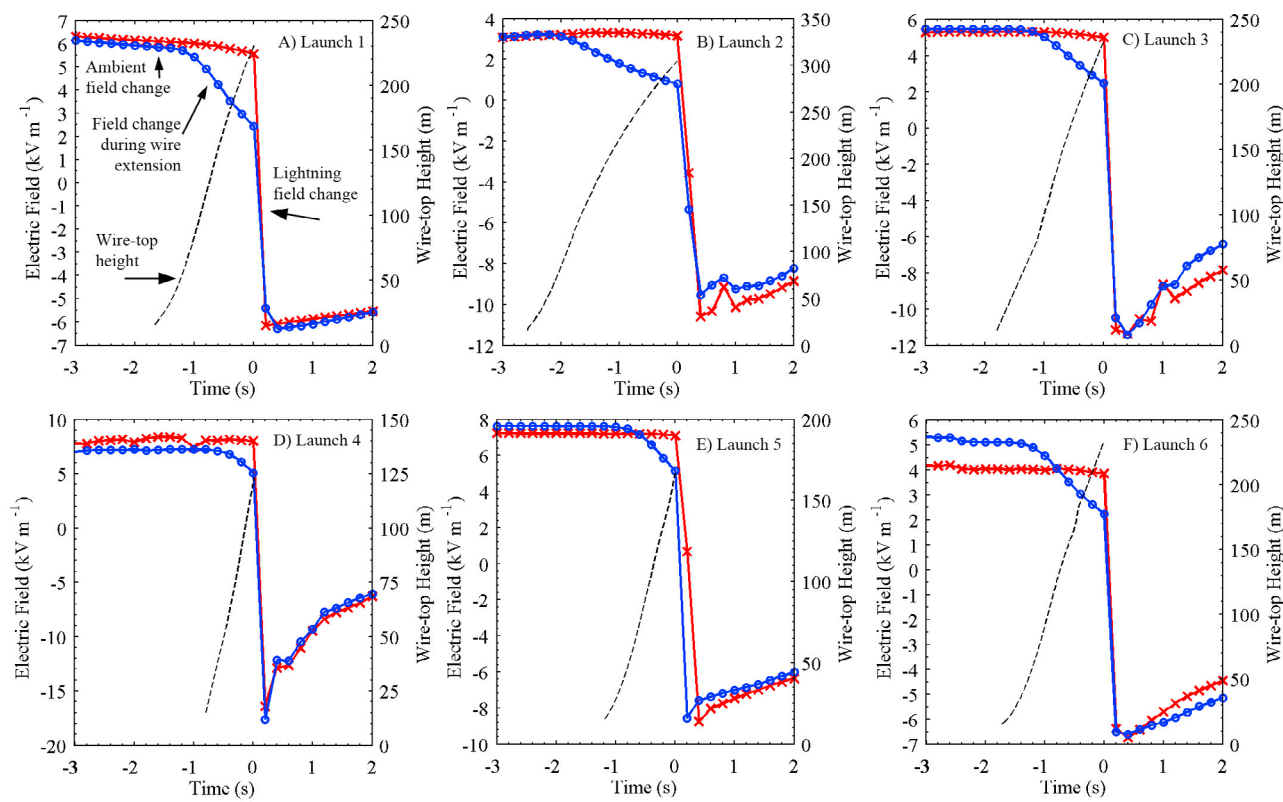


Figure 3. The ground-level electric field changes at 60 m (solid blue line with circles, left vertical scale) and 350 m (solid red line with crosses, left vertical scale) along with the wire-top heights (dashed black line, right vertical scale) versus time. Salient features in the electric field change that are evident in all launches are identified in Figure 3a for Launch 1. In each plot, time zero corresponds to the lightning field change and the last wire-top height measurement.

which can reduce the electric field at ground by up to several tens of V m^{-1} , depending on the charge height and the horizontal distance of the sensor from the wire. If several tens of precursors occur during the wire ascent, the cumulative ground-level electric field change from precursors is significant, and the total electric field reduction at ground during the wire ascent is then a combination of the presence of the induced wire charge and the precursor charge in the surrounding air.

3. Data

[18] This section begins with a description of the wire-height measurements. Next, we present measurements taken during six wire launches showing how the ground-level electric field varies with time as the grounded wire is extended vertically, and then we examine the field change versus wire height. Finally, we describe our measurements of the precursor currents and the corresponding ground-level electric field changes.

3.1. Rocket Height and Wire Extension Rate

[19] The triggering wires were unspooled from the bottom of rockets that are about one meter in length, and it is assumed that the wire-top heights (and wire lengths) were the same as the rocket heights. Rocket trajectories were

determined by tracking either the engine plumes or rocket bodies in the high-speed video data. Luminosity at the wire tip from precursors was often evident and was also used to aid in the trajectory measurements. The rockets do not always ascend purely vertically, and lack of tension or excess slack in a wire could cause wire curvature, especially if the wire were blown by the wind. The straightness and tilt of the wires were determined from the optical image data after the luminous wire explosion during the initial stage of the triggered lightning. None of the six wires studied here exhibited a tilt angle of more than a few degrees or had a significant curvature. We estimate that the wire tops did not deviate horizontally from the launch tower more than 10 m. The rocket speeds were similar in all six launches. All heights discussed in this paper are relative to ground level. In Launches 1, 3, 4, and 5, the high speed video camera did not begin recording until the rockets were at heights of 23 m, 79 m, 40 m, and 21 m, respectively. For these four launches, we estimated the rocket heights prior to the time when the high-speed video records began using a modeled trajectory created from the rocket height of Launch 2, which was tracked from 14 to 304 m. The modeled rocket height and wire extension rate (numerical time derivative of the height) versus time are shown in Figures 2a and 2b, respectively. Figure 2c shows the modeled wire extension rate versus the modeled wire height. The rocket in Launch 2

Table 1. Salient Properties of the Quasi-Static Ground-Level Electric Fields Measured Prior to Initiation of Sustained Upward Positive Leader (UPL) of a Classical Triggered Lightning

Launch	Date	Identification ^a	GPS Time (UTC)	Ground-Level Field at Launch (kV m ⁻¹)		Ambient Field- Change Rate Prior to Launch (kV m ⁻¹ s ⁻¹)		Total Field Reduction Between Launch and UPL Initiation (kV m ⁻¹)		Number of Height of First Precursors Precursor (m)		Total Field Reduction From Precursors ^b (kV m ⁻¹)		Total Lightning Field Reduction (kV m ⁻¹)		Rocket Height at UPL		Initiation (m)	
				60 m	350 m	60 m	350 m	60 m	350 m	60 m	350 m	60 m	350 m	60 m	350 m	60 m	350 m	60 m	350 m
1	4 Jun 2009	UF09-15	20:20:09.585791	6.0	6.1	-0.2	-0.2	3.4	0.5	12	153	0.25	0.03	7.9	11.7	230	230	230	230
2	18 Jun 2009	UF09-21	16:45:00.910124	3.2	3.1	0.3	0.2	2.4	0.0	36	229	0.28	0.07	10.3	13.8	304	304	304	304
3	29 Jun 2009	UF09-26	21:18:55.714751	5.5	5.3	0.0	0.0	3.0	0.3	24	168	0.67	0.13	12.9	16.2	232	232	232	232
4	30 Jun 2009	UF09-30	14:01:04.016626	7.2	8.1	0.0	0.0	2.2	0.0	10	79	0.17	0.10	22.7	24.5	123	123	123	123
5	18 Aug 2009	UF09-42	16:24:41.500156	7.6	7.2	0.0	0.0	2.5	0.1	37	83	0.32	0.02	13.7	15.9	161	161	161	161
6	27 Sep 2010	UF10-25	18:34:20.558752	5.1	4.0	0.0	0.0	2.9	0.2	22	147	0.15	0.03	8.8	10.2	233	233	233	233

^aUFxx-yy, where xx is the year and yy is the shot number for that year.^bDistances scaled from E2 measurement at 156 m from wire.

reached a maximum speed of about 160 m s⁻¹ when the rocket was at a height of about 80 m.

3.2. Ground-Level Quasi-Static Electric Field Measurement

[20] The ground-level quasi-static electric field measurements at 60 m and 350 m are coplotted with the rocket height on a 5 s time scale in Figures 3a, 3b, 3c, 3d, 3e, and 3f for Launches 1, 2, 3, 4, 5, and 6, respectively. The salient features in the ground-level electric field change during the triggered lightning are identified in Launch 1 in Figure 3a and summarized in Table 1. These features are apparent to varying degree in all six launches. The precise time alignment of the field mill data to all other data was not straightforward because the field mill data were not recorded with GPS timing. In order to perform the analysis presented in this paper, we assumed that the times when the sustained upward positive leaders began in the high-speed video images (recorded with GPS timing and precise to about 100 μ s) corresponded to the field mill data points at the onset of the relatively large and fast field change associated with the initiation of the sustained upward positive leader of triggered lightning (placed at time zero in the plots of Figure 3). For the data presented in Figure 3, the sustained upward positive leaders may have began any time between 0 s and 0.2 s, and it follows that there is 200 ms timing uncertainty in the analysis.

[21] The following describes the general changes, during the triggering of a lightning flash, in the ground-level electric field within horizontal ranges that are similar to the total height of the triggering wire. Prior to launching the rocket, the ground-level electric field magnitudes at 60 m and 350 m are about the same; they differ at most by 1.1 kV m⁻¹ in Launch 6. Further, the rate of change in the field magnitude before launch at both distances is about the same and relatively low. This fact is primarily a result of launching the wires at the ends of storms when the cloud recharging rate is relatively slow and there is a low natural-lightning flash rate. The maximum rate of ground-level electric field change is 300 V m⁻¹ s⁻¹ in Launch 2 (at 60 m). The similarity in the field magnitudes and rates of change give an indication of the horizontal homogeneity of the electric field and space charge near ground between the two sensors, located 390 m apart.

[22] Shortly after the rocket launch, the ground-level electric field magnitude at 60 m begins to decrease, but apparently not significantly until the wire top has been lifted to a height between 50 and 75 m. The field reduction shape due to the wire shielding at 60 m begins as convex and transitions to concave when the wire top has been lifted to a height of 150 m. This transition is not observed in Launch 4 because the sustained upward positive leader initiated at a height of 123 m. It is not clear if the extending wire causes significant ground-level electric field reduction at 350 m, at least not until the wire reaches an altitude between 150 and 250 m. The field reduction at 350 m during the wire-top ascent was at most 500 V m⁻¹ in Launch 1, but prior to launching the rocket the ground-level electric field reduced at a rate of 200 V m⁻¹ s⁻¹.

[23] In all events, the sustained upward positive leader and initial continuous current produced a large field change (identified in Figure 3a and henceforth referred to as the

Table 2. The Initial Stage (IS) Duration, the Time Interval Between the End of the IS and the First Return Stroke, and the Duration of the Return Stroke Stage^a

Launch	IS Stage Duration (ms)	Time Between IS and First Return Stroke (ms)	Number of Return Strokes	Return-Stroke Stage Duration (ms)
1	161	-	-	-
2	552	-	-	-
3	534	57.6	5	541
4	238	138	1	216
5	630	631	1	199
6	210	-	-	-

^aReturn-stroke stage is the time from the fast rise of the first return-stroke current to the end of the final return-stroke current, including any continuing current. There were no return strokes in Launches 1, 2, and 6.

“lightning field change”) at both 60 m and 350 m. Table 2 presents, for the six triggered lightning flashes, the initial stage (IS) duration, the time interval between the end of the IS and first return stroke (RS), the duration of the return strokes (the time from the first stroke to the end of the final stroke’s current), and total number of return strokes (these times were determined from channel-base current measurement not shown here). The IS durations, as determined from the current records, were always longer than the lightning field change durations that were measured by the field mills, with the exception of Launch 1. The lightning field change was as large as -24.5 kV m^{-1} at 350 m in Launch 4. The lightning field change was always larger at 350 m than at 60 m, and the sum of the field change during the wire ascent and the lightning field change at both distances were similar. After the flash ends, the electric field magnitude at ground ‘recovers’, i.e., begins changing in the positive direction, mainly due to negative space charge generation by corona at ground in response to the sudden onset of negative electric field of large magnitude [e.g., Standler and Winn, 1979; Chauzy and Soula, 1987; Chauzy and Soula, 1989]. Some of the field recovery possibly results from cloud recharging after the triggered lightning. Note that in Figure 3, the rate of field recovery is apparently higher when the maximum field excursion due to the lightning field change is higher.

[24] Figure 4 presents the measured ground-level electric field plotted versus wire-top height for the six launches at distances from the launch tower of 60 m (Figure 4a) and 350 m (Figure 4b). The first data point in each curve corresponds to the electric field value just before the rocket was launched. The last data point represents the ground-level electric field value and rocket height when the sustained UPL began. It is apparent in Figure 4a that the rate of electric field change at 60 m was different in different launches, and the change began mostly after the wire top had reached a height of 50 m. As seen in Figure 4b, the ambient electric field change apparently dominates the total electric field at 350 m from the wire until the wire reached a height between 150 and 250 m, perhaps with the exception of Launch 1. As we will show in section 3.3, some of the measured field change at ground during the wire ascent was due to precursors, particularly at 60 m. Precursor field changes will be accounted for in the modeling (see section 4).

3.3. Precursor Current in the Wire and Corresponding Charge Transfer

[25] Each launch discussed here resulted in triggered lightning in electric fields of positive polarity (negative charge overhead), and thus, precursor charge deposited ahead of the wire tip is of positive polarity, and a current wave carrying an equal amount of negative charge is guided toward ground by the triggering wire. The triggering wire acts like a transmission line that is terminated approximately by short-circuit conditions at ground and open-circuit conditions at the wire tip. Current-wave reflections are produced at the ground and the wire tip, and a combination of transmission line losses (series resistance and shunt conductance) and partial

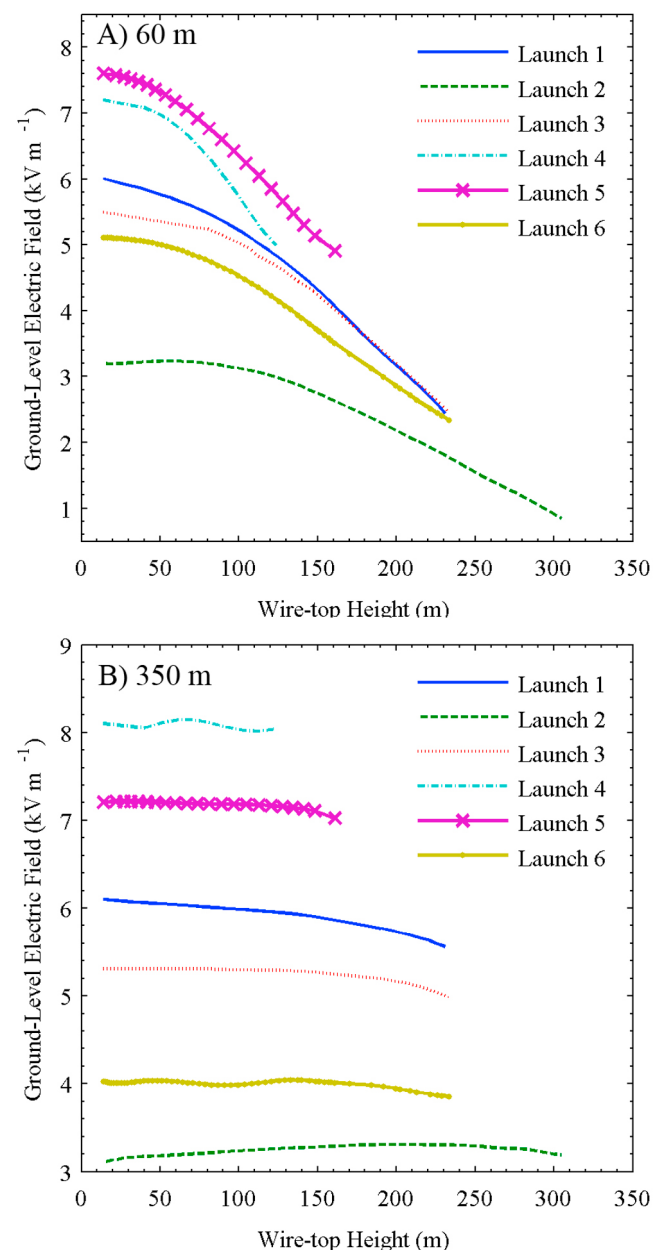


Figure 4. Field change versus wire-top height at (a) 60 m and (b) 350 m. Note that the vertical scales of electric field in the two plots are different.

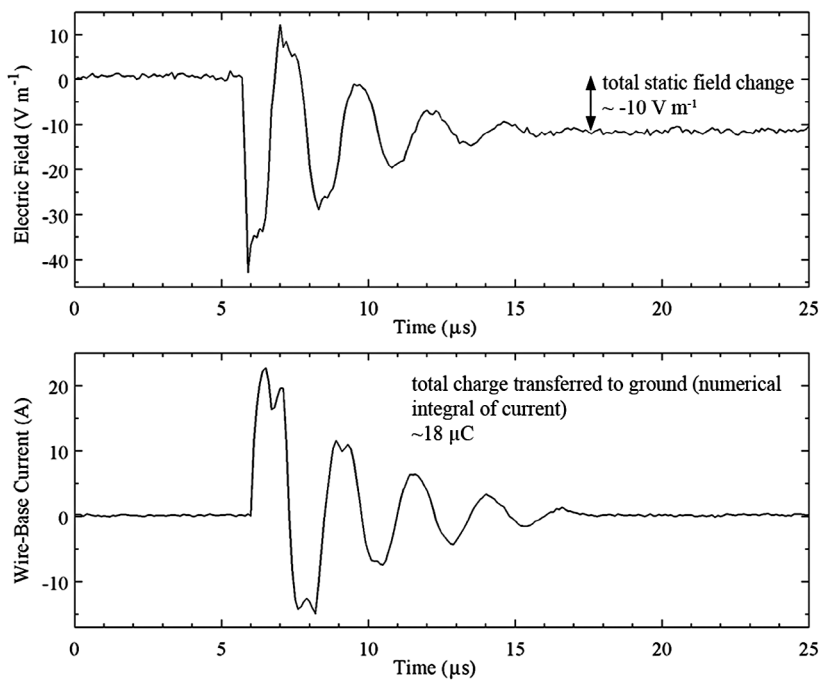


Figure 5. An example of a precursor. (top) The ground-level electric field change measured at 156 m (by E2) but range-scaled by equation (1) to a horizontal distance of 60 m from wire. (bottom) The corresponding wire-base current. The $18 \mu\text{C}$ of negative charge transferred to ground during this precursor produced an overall field change at 60 m of about -10 V m^{-1} .

absorption at the wire ends decrease the current magnitude with each reflection. Thus, precursor current signatures take the form of a damped oscillatory pulse. The propagation of the current wave on the wire radiates a similarly shaped damped oscillatory field signature, and a “static” field change at ground is produced from the overall lowering of negative charge from the wire tip to ground. Figure 5 presents examples of precursor current and electric field signatures on a $25 \mu\text{s}$ time scale that transferred about $18 \mu\text{C}$ of negative charge from a height of 152 m to ground, and produced a ground-level electric field change of about -10 V m^{-1} at a distance of 60 m from the wire.

[26] In the comparisons between measured and modeled field changes during the wire ascents, the field changes from precursors are first removed from the measured ground-level field change. It is assumed here that precursor charge can be represented by a point source at the wire tip. Of the six launches analyzed here, both the wire-base currents and fast electric field changes were adequately measured in Launches 1 and 6. For these two launches, the field change of each precursor at 60 m and 350 m is inferred from the following approximation [Uman, 1969, equation (3.3)]:

$$\Delta E = \frac{2\Delta QH}{4\pi\epsilon_0(H^2 + R^2)^{3/2}}, \quad (1)$$

where ϵ_0 is the permittivity of free space, H is the wire-tip altitude, R is the horizontal distance between the wire base (launch tower) and the electric field sensor, and ΔQ is the total charge transferred to ground, found by numerically integrating the precursor current. Additionally, equation (1) was used to scale the precursor field changes measured

by E2 at a range of 156 m to field change at ranges of 60 m (e.g., Figure 5, top) and 350 m. For Launches 2 through 5, the current measurement saturated at about 20 A, and the first current peaks of most precursors saturated, making it impossible to determine ΔQ from integrating the precursor current at the wire bottom, so the measured field changes from E2 were used to determine ΔQ via equation (1). The placement of a plastic dome over the E2 sensor to shield it from rain introduced uncertainty to the sensor’s amplitude calibration, so we calibrated the measured field changes from E2 to the inferred field change (using equation (1)) from accurate wire-base current measurements for 96 precursors in four launches: Launches 1, 6, and two launches otherwise not analyzed here (different than Launches 1 through 6): one on 26 May 2009 and the other on 4 June 2009 (the latter was in the same storm of Launch 1). According to this calibration, the E2 measurements were consistently too high in amplitude by 29%. Table 3 presents for the 96 precursor current pulses statistics on the total

Table 3. Salient Statistics of Precursor Charge and Electric Field Change^a

	Charge Lowered to Ground (μC)	Field Reduction at 60 m ^b (V m^{-1})
Arithmetic Mean	33.9	27.1
Standard Deviation	23.5	16.0
Geometric Mean	26.9	22.2
Median	27.8	24.0
Minimum	4.8	4.2
Maximum	151.7	86.9

^aSample size of 96.

^bDistance scaled from E2 measurement at 156 m from wire.

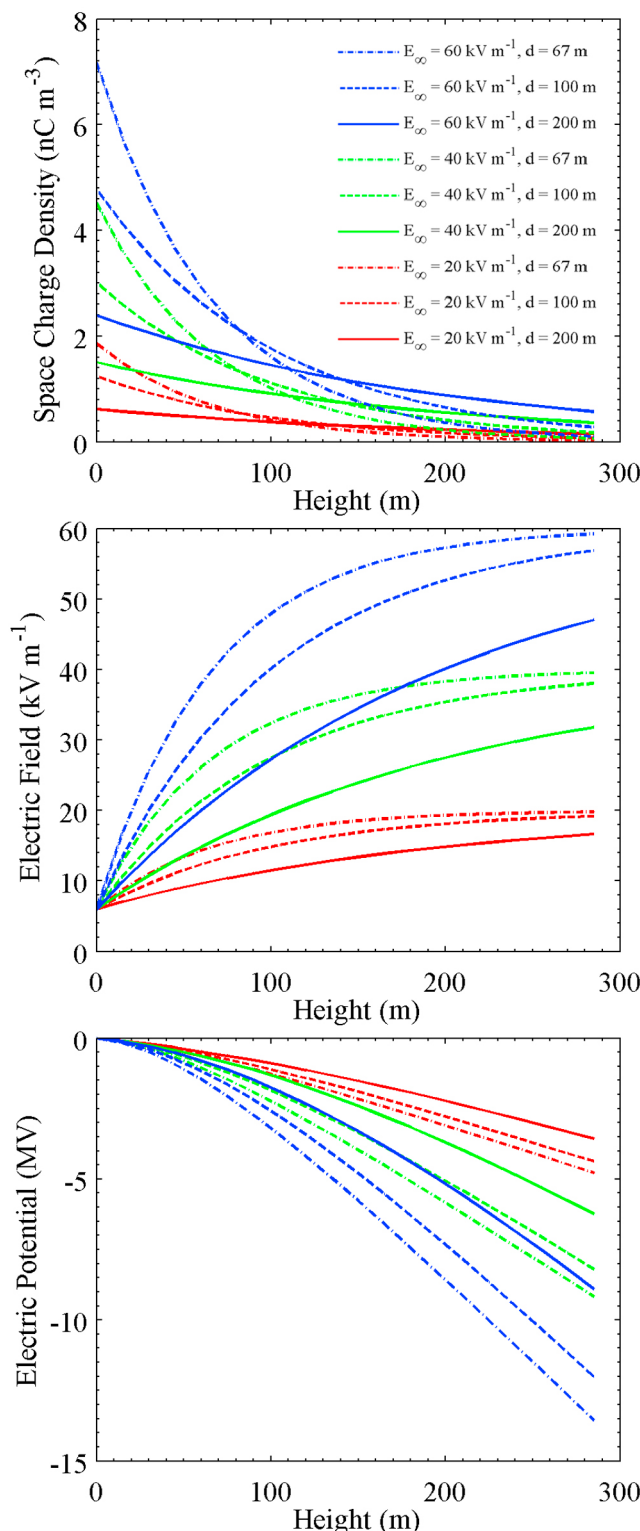


Figure 6. The vertical profiles of (top) space charge density, (middle) electric field magnitude, and (bottom) electric potential, computed using equations (2), (3), and (4), respectively, for the nine combinations of d and E_∞ values and $E_0 = 6 \text{ kV m}^{-1}$. A common legend is shown on the top plot.

negative charge lowered to ground and E2-measured electric field change scaled to 60 m. There was no correlation between the amount of precursor charge deposited ahead of the wire tip and wire-tip height.

4. Modeling

[27] This section begins with a description of the model construct and the assumed vertical profiles of space charge density, electric field intensity, and electric potential. We present examples of possible model outputs, and then determine which model parameters yield electric field change predictions that best fit the measured electric field changes, thereby inferring vertical profiles of space charge density, electric field intensity, and electric potential. Finally, we examine the model predictions of the radial electric field along the wire as a function of height for Launch 1.

4.1. Model Description

[28] The electric field structure is assumed to have cylindrical symmetry centered on the vertical wire, allowing the three-dimensional field structure to be modeled in two dimensions. The triggering wire is infinitely thin in the model. The model domain is a square ‘slice’ of the three-dimensional space, with the left side being the axis of symmetry. The following five conditions are imposed: (1) the total vertical and horizontal (radial) extent of the model space each is 3 km, (2) the vertical wire extension begins in the lower left corner at ground, and continues up along the left boundary, (3) the boundaries at ground (bottom side) and along the wire are at zero potential, (4) the horizontal (radial) derivative of the electric potential (the negative of the radial electric field) is zero on the right boundary and on the left boundary vertically above the wire top, and (5) the potential along the top boundary (at $z = 3 \text{ km}$) is defined by equation (4) (described below).

[29] We assume an exponentially decaying space charge density profile versus altitude. This choice was based primarily on the rocket soundings of the electric field versus height with relatively high spatial resolution that were presented in the work of Willett *et al.* [1999], and an exponentially decaying space charge density profile is the simplest realistic profile with the minimum number of free parameters to test in the computationally intensive model. Prior to launching the rocket, the height profiles of the exponentially decaying space charge, the corresponding electric field as a function of z , and the electric potential as a function of z are described by the following three relations, respectively:

$$\rho(z) = \varepsilon_0 \frac{\exp(-z/d)}{d} (E_\infty - E_0), \quad (2)$$

$$E(z) = E_\infty - \exp(-z/d) (E_\infty - E_0), \quad (3)$$

$$V(z) = d(E_\infty - E_0) [1 - \exp(-z/d)] - E_\infty z. \quad (4)$$

The equations for $\rho(z)$ and $V(z)$ are consistent with the equation for $E(z)$ via Gauss’s Law $\rho(z) = \partial \varepsilon_0 E(z) / \partial z$ and the definition of the electric potential $V(z) = - \int_0^z E(z') dz'$, respectively.

[30] The two adjustable parameters of the model are: the rate of charge decrease with height (e-folding length) d and

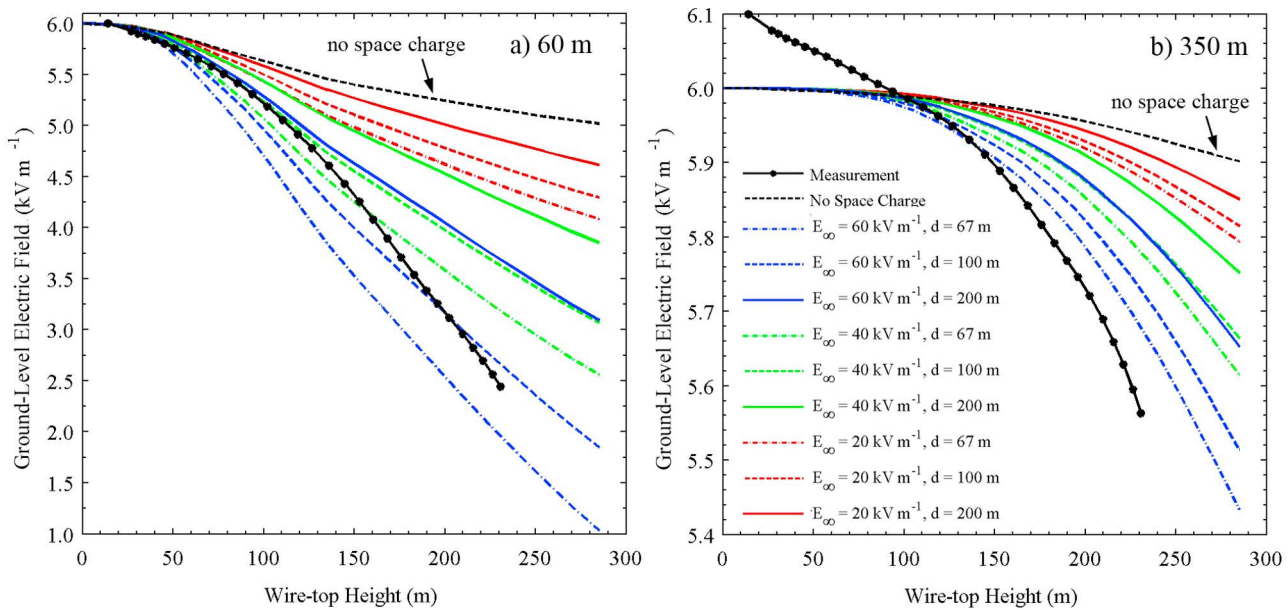


Figure 7. The model-predicted ground-level field change at (a) 60 m and (b) 350 m for no space charge and the nine cases of exponentially decaying space charge density for $E_0 = 6 \text{ kV m}^{-1}$, with a common legend shown in Figure 7b. The measured field change for event 060409-2 at both distances is shown for comparison. Note the different vertical scales of electric field in Figures 7a and 7b.

the electric field magnitude far above the space charge layer E_∞ . The ground-level electric field when the wire is first launched, E_0 , is a measured value. The electric potential is found first by numerically solving Poisson's equation (or Laplace's equation for the zero space charge case) using the finite element method. The electric field is then found by taking the negative of the gradient of the electric potential. The initial finite element mesh was refined many times using higher-order finite elements with the most grid points located near ground and along the left boundary where the wire was placed.

[31] Because of the computationally intensive nature of our Poisson solver, we ran the model for only three values each of the two free parameters, E_∞ (20, 40 and 60 kV m^{-1}) and d (67, 100 and 200 m), as well as the zero space charge case (d is set to zero), for the six initial measured ground-level electric field values E_0 (ranging from 3.2 to 7.6 kV m^{-1}). For example, Figure 6 presents $\rho(z)$, $E(z)$, and $V(z)$ for the nine combinations of E_∞ and d and $E_0 = 6 \text{ kV m}^{-1}$. For the zero space charge case, the electric field prior to launching the rocket is vertical and is equal to the measured field at the ground E_0 for all z . We then chose the solution that provided the best least squares fit to the time series of electric field measured at the 60 m range.

4.2. Model Predictions

[32] Figure 7 presents the model-predicted, ground-level electric field change at 60 m (Figure 7a) and 350 m (Figure 7b) for the zero space charge case and for the nine cases of exponentially decaying space charge, all for $E_0 = 6 \text{ kV m}^{-1}$. The corresponding measurements for Launch 1 are also shown (although the E_0 value at 350 m was about 6.1 kV m^{-1} versus 6 kV m^{-1} assumed in calculations). The model-predicted ground-level electric field change is lowest when

zero space charge was assumed: about -1 kV m^{-1} at 60 m and -100 V m^{-1} at 350 m. The second-smallest predicted ground-level field change is for the lowest space charge density at ground (corresponding to highest $d = 200 \text{ m}$ and smallest $E_\infty = 20 \text{ kV m}^{-1}$): about -1.4 kV m^{-1} at 60 m and 0.1 kV m^{-1} at 350 m. The largest model-predicted field change is for the highest space charge density at ground (corresponding to smallest $d = 67 \text{ m}$ and highest $E_\infty = 60 \text{ kV m}^{-1}$): about -4.9 kV m^{-1} and -0.5 kV m^{-1} at 60 m and 350 m, respectively. In all of the predicted ground-level field changes at 60 m for zero space charge and the nine combinations of E_∞ and d , there is a point of inflection when the wire top reaches a height of about 130 m. An inflection point is not evident in the modeled field change curves at 350 m, although presumably there would be one if the wire reached a height of 700 m.

4.3. Model Fit

[33] Figures 8a–8f present, for Launches 1, 2, 3, 4, 5, and 6, respectively, the original measured field change at 60 m, the measured field change with the precursor field changes removed (referred to as the precursor-adjusted measurement), and also the model prediction that best matches the precursor-adjusted measurement according to the best least squares fit. The values of E_0 (assumed to be equal to the measured value), E_∞ , and d corresponding to the best fitting model predictions, along with the space charge density at ground are given in each plot. For each of the plots in Figure 8, a vertical arrow points to the height at which the first precursor field change was removed from the measurement. Below these heights the original measured curves and the precursor-adjusted measured curves are identical. In each launch, the overall field change from precursors, several hundred V m^{-1} , is small relative to the overall field

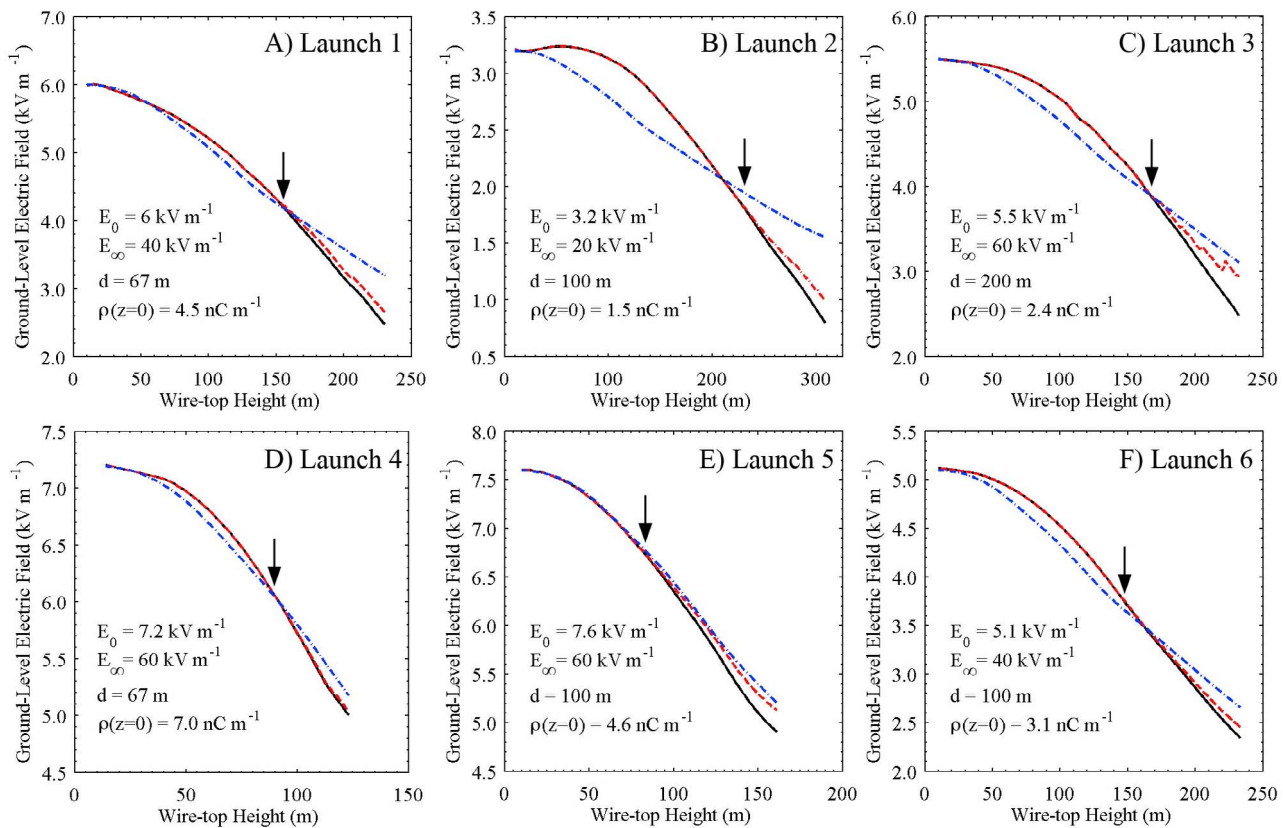


Figure 8. The measured field change at 60 m (solid black line), the precursor-adjusted measurement (dashed red line), and the model-predicted field change that best matches the precursor-adjusted measurement according to the least squares norm (dash-dotted blue line). The values of E_0 (assumed to be equal to the measured value), E_∞ , d , and $\rho(z=0)$ (the space charge density at ground) corresponding to the best model fit are shown in the bottom left of each plot. Note that the plots have different height and electric field scales. The vertical arrows point to the wire-top height at which the first precursor is removed.

change due to the wire shielding effect, several kV m^{-1} . The field adjustments for precursors appear as positive-going steps, although the field change for many precursors is too small to be evident in the plots of Figure 8. Accounting for precursor field changes has the effect of reducing the total field change. Table 4 summarizes the parameters that produced the best fitting model predictions for each launch, as well as the model predictions of ground-level space charge density, the ambient vertical electric field for the height at which the sustained UPL initiated (these heights are given in Table 1), and the electric potential traversed by the wire.

The modeling results indicate that the ambient electric field at the wire-tip height was lower and the electric potential traversed by the wire was larger when the sustained UPL initiated at higher altitudes. No attempt was made to fit modeled electric field changes to the measured electric field changes at 350 m since any wire-shielding effect at this distance was not clearly observable.

4.4. Model Predicted Wire Surface Charge

[34] In addition to predicting the ground-level electric field, the model yields the vertical (z component) and radial

Table 4. Model Parameters That Produced Model Predictions That Best Fit the Precursor-Adjusted Measurement of Ground-Level Electric Field at 60 m and the Corresponding Space Charge Density at Ground, and the Electric Field and the Electric Potential at the Triggering Height According to Equations (2), (3), and (4)^a

Launch	E_0^b (kV m^{-1})	E_∞ (kV m^{-1})	d (m)	$\rho(z=0)$ (nC m^{-3})	E at Triggering Height (kV m^{-1})	V at Triggering Height (MV)
1	6.0	40	67	4.5	39	-4.1
2	3.2	20	100	1.5	19	-3.0
3	5.5	60	200	2.4	43	-3.9
4	7.2	60	67	7.0	51	-2.3
5	7.6	60	100	4.6	50	-1.3
6	5.1	40	100	3.1	36	-3.2

^aSee section 4.3.

^bAt a distance of 60 m from the launch tower, equal to the measured value.

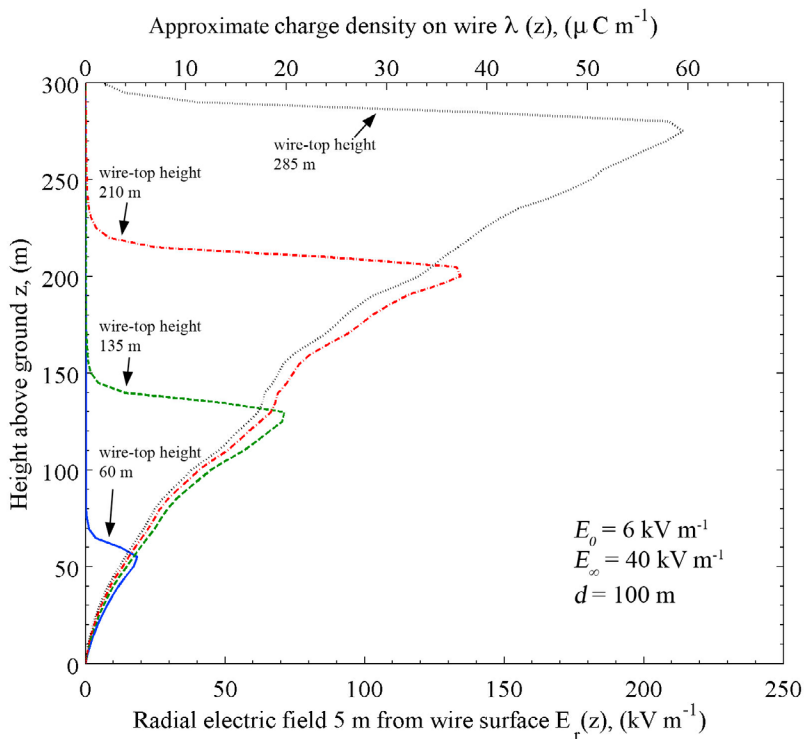


Figure 9. Examples of the model-predicted height profiles of the radial electric field 5 m from the wire (bottom axis) and equivalent approximate line charge density (top axis). Each curve is a ‘snapshot’ of the radial electric field and charge density along the wire when the wire top is at a certain height. The calculated radial electric field varies as $1/r$ from 10 m to the wire’s surface in the assumed absence of corona, except near the top of the wire. The induced charge densities (top scale) are inferred from the radial electric field (bottom scale) using Gauss’s law: values of charge density near the wire top are underestimated because there is vertical component of electric field not taken into account in these calculations (see discussion in section 4.4). The radial field does not drop to zero above the maximum wire-top height because there is some radial component of electric field above the wire at a radial distance of 5 m (one would expect a purely vertical field only along the wire’s longitudinal axis).

electric field near the surface of the wire. From these fields, we can infer the corresponding charge per unit length that must exist on the wire and/or corona sheath as a function of height. Figure 9 presents examples of the model-predicted height profiles of the radial electric field along the wire at a radius of 5 m (bottom axis) and the approximate charge density (top axis) that must exist along the wire to produce the radial electric field according to Gauss’s Law when the input parameters were $E_\infty = 40 \text{ kV m}^{-1}$ and $d = 100 \text{ m}$, and $E_0 = 6 \text{ kV m}^{-1}$. Each of the four curves in Figure 9 is the model-predicted radial electric field and corresponding charge per unit length from 0 m to 300 m at four different times, when the wire top was at heights of: 60 m, 135 m, 210 m, and 285 m. The charge per unit length is calculated as follows. A Gaussian cylinder of a few meters height and a few meters radius has its axis collocated with the wire, and $\epsilon_0 \vec{E}$ is integrated over the lateral surface of the cylinder to yield the charge inside the cylinder. For all locations of the Gaussian cylinder, except at the top of the wire, the electric flux out the top and bottom circular surfaces is negligible, leading to a charge per unit length $\lambda = 2\pi\epsilon_0 r E_r$ (top axis of Figure 9), where E_r is found to vary as r^{-1} out to about 10 m. At the top of the wire, the electric flux out the top surface of the Gaussian cylinder is of the same order of magnitude as

the flux out the cylindrical side surface, so the actual charge per unit length at the top of the wire is two or three times that plotted in Figure 9. The exact value determined depends on the grid size of the model calculations, which has a practical lower limit.

[35] The model predicts that the radial electric field magnitude and charge density at any given height are highest when the wire first reaches that height, thereafter decreasing slightly as the wire continues ascending. The model-predicted radial electric field (at $r = 5 \text{ m}$) and charge density (underestimated near the wire tip) shown in Figure 9 reach maxima of about 210 kV m^{-1} and $60 \mu\text{C m}^{-1}$, respectively, at a height of 270 m when the wire top is at 285 m. The model predicts that the radial electric field near the wire and corresponding charge per unit length increases with increasing values of E_∞ and decreasing values of d . Note that the nonsmooth nature of the curves is due to unevenly spaced finite element mesh points.

[36] The model predicts that there is a total charge along the wire of about 6.5 mC when the wire top is at a height of 285 m. The current required to supply the charge (the rate of change of total charge on wire as the wire extends upward) increases steadily as the wire ascends to a height of 135 m, reaching a level of about 3 mA , and continues to increase for

higher wire heights, although at a slower rate because the wire extension rate is decreasing (see Figure 2).

[37] The model predicts that the radial electric field magnitude is highest about 10 m below the top of the wire. The predicted decrease of radial electric field in the upper 10 m or so of wire is due to the electric field becoming more vertical, and less radial, near the wire top. The radial field does not drop to zero above the maximum wire-top height because there is some radial component of electric field above the wire at a radial distance of 5 m (there should be radial electric field everywhere except directly along the wire axis), and to some extent because of insufficient mesh refinement. The model predicts that the vertical electric field at 5 m radius increases from small compared to the radial field some meters below the wire top to a maximum at the wire top, above which the z-directed field decreases.

5. Analysis and Discussion

[38] Our measurements of the ground-level electric field change during the vertical extension of a thin, grounded wire are similar to previous reports. Willett *et al.* [1999] reported higher-magnitude but similarly shaped field changes at a distance of about 30 m from their launcher, or half the distance at which we measured field changes. For their 'flight 6' [Willett *et al.*, 1999, Figure 6], they reported that the electric field began at about 7 kV m^{-1} and the field changed during the wire extension (up to 307 m) by a little over -7 kV m^{-1} , becoming slightly negative before the UPL initiated. Our largest measured field change during a wire extension was -3.4 kV m^{-1} for Launch 1. The lightning field change of 'flight 6' of Willett *et al.* [1999] was about -7 kV m^{-1} , and the combined field change from the wire ascent and triggered lightning was about -14 kV m^{-1} . Liu *et al.* [1994] reported a similar quasi-static electric field change signature measured 75 m from the launcher during a triggering attempt with positive charge overhead. The field change during the wire ascent was about 3.5 kV m^{-1} [Liu *et al.*, 1994, Figure 2].

[39] Figure 10 presents a scatterplot of the ground-level electric field magnitude when the wire-trailing rocket was launched versus the height at which the sustained UPL developed (triggering height). The two quantities show a strong linear relationship with a correlation coefficient of -0.85 . Hubert *et al.* [1984] reported a strong power law relationship (correlation coefficient of -0.82) between the triggering heights (from about 100 to 600 m) and ground-level electric field magnitudes (between 4 and 13 kV m^{-1}) for 35 triggered flashes in Langmuir Laboratory in New Mexico. The power law relation of Hubert *et al.* [1984] is also shown in Figure 10 (they did not report data points). The results in Figure 10 indicate that for the same electric field at ground lightning can be triggered at a lower triggering height at the ICLRT than at Langmuir Laboratory. In explanation of these observations, there may have been less space charge present in the vicinity of the triggering experiments at Langmuir than at the ICLRT, or the electric field magnitudes of Hubert *et al.* [1984] may have been enhanced by the mountainous local topography. It is worth noting that Horii and Nakano [1995] reported for winter triggered-lightning studies at Kahokugata site in Japan that no clear correlation was observed between the triggering

height and the initial ground level electric field for either positive or negative lightning polarity.

[40] The highest number of precursors preceding the sustained upward leader in the data presented was 37 in Launch 5. There were other launches that were not included in this analysis because the precursor activity was extraordinarily high, with current pulses occurring every $100 \mu\text{s}$ or so, and we have not developed a method by which to measure the charge transfer and field change from the hundreds to thousands of precursor current pulses that occurred in these relatively unusual wire launches. The sum of the precursor field changes in these events could well be larger than the field change from the induced charge on the ascending wire.

[41] As seen in Figure 8, there is good agreement between the model-predicted and precursor-adjusted measured ground-level electric field at 60 m from the wire, when an exponentially decaying space charge profile is assumed, particularly in Launches 1, 4 and 5. There is nearly perfect agreement between measurement and model for Launch 5. Interestingly, there was a 1 cm air gap in the ground lead for Launch 5, although it is unclear how the measurement would differ if the air gap were not present. The rate at which the measured electric field magnitude initially decreases is well modeled for Launches 1, 4 and 5. For Launches 2 and 3, the measured field change when the wire is at a higher altitude is larger than the model predicts. This discrepancy could well be due to the uncertain time alignment between the rocket trajectory and ground level field change. As noted in section 3.2, we assumed that the sustained upward positive leaders began when the lightning field changes in the field mill records began (time zero in the plots of Figure 3). However, the sustained upward positive leaders may have begun between 0 s and 0.2 s, introducing an uncertainty of 200 ms in the data time alignment. The timing uncertainty means that the wire may have been launched up to 200 ms later than was assumed in the present analysis and the computed field versus height curves may be shifted horizontally to lower wire-top heights. For example, in Launch 2 the electric field increases (in Figures 4 and 8) for wire-top heights from about 14 m to 60 m. The 200 ms timing uncertainty allows the wire launch to begin when the field maximum occurred, in which case there would probably be a better match of the model prediction to the measurement, although perhaps for a different space charge profile.

[42] The radial electric field of the model-predicted line charge along the wire is large enough to produce corona. As noted in section 2.1, the wire has a diameter of $2 \times 10^{-4} \text{ m}$, and if the minimum electric field strength necessary to produce corona is assumed to be 1 MV m^{-1} [e.g., Kodali *et al.*, 2005; Maslowski and Rakov, 2006], then a line-charge density as low as 11 nC m^{-1} will produce corona. For a line-charge density of $60 \mu\text{C m}^{-1}$ (the maximum model prediction shown in Figure 9), the radial electric field drops below 200 kV m^{-1} (the minimum electric field for corona propagation according to Griffiths and Phelps [1976]) for a radius of about 5.4 m. The model indicates that for all wire launches, the induced charge on the wire expanded radially via corona on the order of 5 meters. However, the location of the wire/corona-sheath charge does not affect the model predictions as long as that corona sheath charge magnitude is essentially the same as would be found on the wire (or on a grounded wire of any radius) in the absence of corona. It is possible that

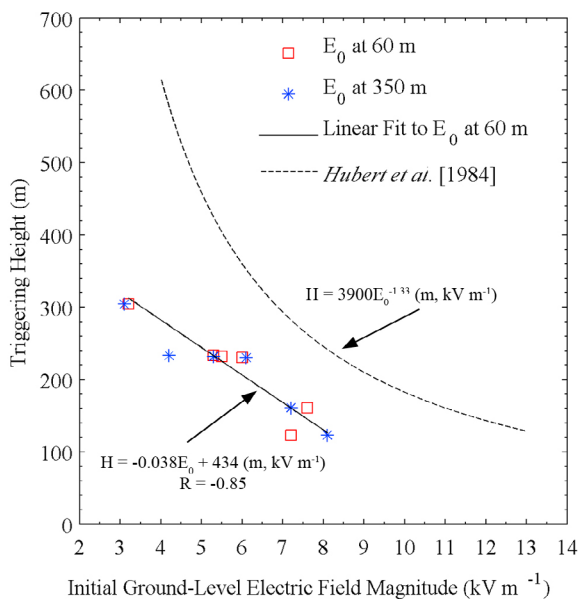


Figure 10. Triggering height versus initial ground-level electric field magnitude.

wind advection or conduction current removes a part of the charge created by corona from the vicinity of the wire, in which case corona resupplies the removed charge with additional charge. The removed charge would then be supplementary to the charge required to keep the wire at ground potential, and would enhance the overall electric field decrease measured at ground beyond what the model would predict (after accounting for precursor charge). The supplementary charge effect may explain some of the divergence of the model predictions and precursor-adjusted measurements of electric field change that typically begins around the wire heights when the first precursor begins (see Figure 8).

[43] Another possible source of supplementary charge is the rocket motor exhaust, as previously suggested by *Fieux et al.* [1978]. The rocket motors used in our experiments are specified to have a 1.2 s burn time, or about half the typical time the wire ascends before triggering lightning (see Figure 3). We view any charge deposition by the motor exhaust as having negligible effect on our measurements for the following reason: If charge deposition by the motor exhaust were significant, one would expect a discontinuity in the measured field reduction during the wire extension when the motor extinguishes at a time 1.2 s after launching the wire; such discontinuities are not observed.

[44] Our choice of an exponentially decaying space charge density, and the parameters E_∞ and d were based on the rocket soundings of the vertical electric field versus altitude in the work of *Willett et al.* [1999]. The rocket soundings of *Willett et al.* [1999] indicated that the electric field aloft increased exponentially with height up to heights of tens to hundreds of meters, above which it became more or less constant. All other reports of measurements of the electric field aloft found in the literature indicate it increases with height, although not necessarily exponentially. The true space charge profiles through which the wires ascended may not have varied with height exponentially, or even mono-

tonically. Further, our model solutions are not unique to the space charge profiles we assumed; other space charge density profiles versus height may yield similar or better model predictions. The nonunique nature of the model predictions is obvious in Figure 7, which shows that the model-predicted ground-level electric field change with $d = 100$ m and $E_\infty = 40$ kV m⁻¹ is nearly the same as the model prediction with $d = 200$ m and $E_\infty = 60$ kV m⁻¹. In fact, for Launch 3, the model prediction with $E_\infty = 60$ kV m⁻¹ and $d = 200$ m fits the measurement only slightly better than the model prediction with $E_\infty = 40$ kV m⁻¹ and $d = 100$ m. Similarly, for Launch 6, the model prediction with $E_\infty = 40$ kV m⁻¹ and $d = 100$ m fits the measurement only slightly better than the model prediction with $E_\infty = 60$ kV m⁻¹ and $d = 200$ m.

[45] The good agreement between the model-predicted field change and precursor-adjusted measured field change, especially for Launches 1, 4 and 5, indicates that our assumptions regarding the uncertainties in the inter-measurement timing, supplementary charge creation along the wire, and the exponentially decaying space charge profiles are not grossly inaccurate. Our analysis at least shows that the triggering wires extended through space charge layers of significant density, such that the atmospheric electric field increased significantly with height. For example, for Launch 1, E_0 was 6 kV m⁻¹, the wire reached a height of 230 m before the sustained upward positive leader began, and the wire caused a ground-level electric field change of -3.2 kV m⁻¹. The model-predicted ground-level electric field change for the same E_0 and wire height (see Figure 7) with zero space charge was only about -700 V m⁻¹, or a factor of four less than the measured field change.

[46] In future experiments, the data quality will be improved by recording all data (including field mill data) with GPS timing, and by measuring low-level wire base currents down to the milliamperes, or even microamperes range. The low-level currents will be measured (our experiment's lower limit was 1 A) in order to test the hypothesis suggested by E. P. Krider (private communication, 2011) that the ambient vertical electric field profile can be determined from the wire-base current versus time, the initial field at ground, and modeling. Additionally, the uniqueness of the model solution will be further constrained with the addition of multiple measurements of the electric field change at different close distances. Comparing model solutions with different assumed space charge profiles may also prove valuable. The modeling will be extended to include the upward positive leader development so as to infer its charge density and propagation speed.

[47] Making inferences of the space charge density and electric field using the presented technique may prove useful in determining when to attempt to trigger lightning, and/or when a ground-based electric field measurements of lightning processes and cloud electric fields may be inaccurate due to the space charge near ground. The inferences may be useful even if they are limited to a few tens of meters above ground. Quickly raising a grounded wire to a few tens of meters above ground may be possible without the use of expensive and potentially dangerous explosive-fueled rockets. We are exploring for future atmospheric electricity experiments (other than triggering lightning) alternative methods of vertically extending grounded wires such as using crossbows and using rockets propelled by pressurized gas.

[48] **Acknowledgments.** This research was partially supported by DARPA grants HR0011-08-1-0088 and HR0011-1-10-1-0061, NSF grant ATM 0852869, and NASA grant NNK10MB02P. Appreciation is owed to Julia Jordan and Mike Stapleton, who assisted in experimental setup, maintenance, and data gathering.

References

Biagi, C. J., D. M. Jordan, M. A. Uman, J. D. Hill, W. H. Beasley, and J. Howard (2009), High-speed video observations of rocket-and-wire initiated lightning, *Geophys. Res. Lett.*, **36**, L15801, doi:10.1029/2009GL038525.

Chauzy, S., and P. Raizonville (1982), Space charge layers created by coronae at ground level below thunderclouds: Measurements and modeling, *J. Geophys. Res.*, **87**(C4), 3143–3148.

Chauzy, S., and S. Soula (1987), General interpretation of surface electric field variations between lightning flashes, *J. Geophys. Res.*, **92**(D5), 5676–5684.

Chauzy, S., and S. Soula (1989), Ground coronae and lightning, *J. Geophys. Res.*, **94**(D11), 13,115–13,119.

Chauzy, S., and S. Soula (1999), Contribution of the ground corona ions to the convective charging mechanism, *Atmos. Res.*, **51**, 279–300, doi:10.1016/S0169-8095(99)00013-7.

Chauzy, S., J.-C. Medale, S. Prieur, and S. Soula (1991), Multilevel measurement of the electric field underneath a thundercloud: 1. A new system and the associated data processing, *J. Geophys. Res.*, **96**(D12), 22,319–22,326.

Fieux, R. P., C. H. Gary, B. P. Hutzler, A. R. Eybert-Berard, P. L. Hubert, A. C. Meesters, P. H. Perroud, J. H. Hamelin, and J. M. Person (1978), Research on artificially triggered lightning in France, *IEEE Trans. Power Apparatus Syst.*, **82**(3), 725–733.

Griffiths, D. J. (1981), *Introduction to Electrodynamics*, Prentice Hall, Englewood Cliffs, N. J.

Griffiths, R. F., and C. T. Phelps (1976), The effects of air pressure and water vapor content on the propagation of positive corona streamers and their implications to lightning initiation, *Q. J. R. Meteorol. Soc.*, **102**, 419–426, doi:10.1002/qj.49710243211.

Horii, K., and M. Nakano (1995), Artificially triggered lightning, in *Handbook of Atmospheric Electrodynamics*, vol. 1, edited by H. Volland, pp. 151–166, CRC, Boca Raton, Fla.

Hubert, P., P. Laroche, A. Eybert-Berard, and L. Barret (1984), Triggered lightning in New Mexico, *J. Geophys. Res.*, **89**(D2), 2511–2521.

Kodali, V., V. A. Rakov, M. A. Uman, K. J. Rambo, G. H. Schnetzer, J. Schoene, and J. Jerauld (2005), Triggered lightning properties inferred from measured currents and very close electric fields, *Atmos. Res.*, **75**, 335–376.

Lalande, P., A. Bondiou-Clergerie, P. Laroche, A. Eybert-Berard, J.-P. Berlandis, B. Bador, A. Bonamy, M. A. Uman, and V. A. Rakov (1998), Leader properties determined with triggered lightning techniques, *J. Geophys. Res.*, **103**(D12), 14,109–14,115, doi:10.1029/97JD02492.

Liu, X., C. Wang, Y. Zhang, Q. Xiao, D. Wang, Z. Zhou, and C. Guo (1994), Experiment of artificially triggered lightning in China, *J. Geophys. Res.*, **99**(D5), 10,727–10,731, doi:10.1029/93JD02858.

Maslowski, G., and V. A. Rakov (2006), A study of the lightning channel corona sheath, *J. Geophys. Res.*, **111**, D14110, doi:10.1029/2005JD006858.

Qie, X., S. Soula, and S. Chauzy (1994), Influence of ion attachment on the vertical distribution of the electric field and charge density below a thunderstorm, *Ann. Geophys.*, **12**, 1218–1228, doi:10.1007/s00585-994-1218-6.

Rakov, V. A., and M. A. Uman (2003), *Lightning: Physics and Effects*, Cambridge Univ. Press, New York.

Soula, S., and S. Chauzy (1991), Multilevel measurement of the electric field underneath a thundercloud: 2. Dynamical evolution of a ground space charge layer, *J. Geophys. Res.*, **96**(D12), 22,327–22,336, doi:10.1029/91JD02032.

Standler, R. B., and W. P. Winn (1979), Effects of coronae on electric fields beneath thunderstorms, *Q. J. R. Meteorol. Soc.*, **105**, 285–302, doi:10.1002/qj.49710544319.

Toland, R. B., and B. Vonnegut (1977), Measurement of maximum electric field intensities over water during thunderstorms, *J. Geophys. Res.*, **82**(3), 438–440, doi:10.1029/JC082i003p00438.

Uman, M. A. (1969), *Lightning*, McGraw-Hill, New York.

Uman, M. A., et al. (1996), 1995 Triggered lightning experiment in Florida, paper presented at 10th International Conference on Atmospheric Electricity, Int. Comm. on Atmos. Electr., Osaka, Japan.

Willett, J. C., D. A. Davis, and P. Laroche (1999), An experimental study of positive leaders initiating rocket-triggered lightning, *Atmos. Res.*, **51**, 189–219, doi:10.1016/S0169-8095(99)00008-3.

C. J. Biagi, J. D. Hill, D. M. Jordan, T. Ngin, V. A. Rakov, and M. A. Uman, Department of Electrical and Computer Engineering, University of Florida, 215 Larson Hall 33, PO Box 116130, Gainesville, FL 32611-6130, USA. (biagi@ufl.edu)

J. Gopalakrishnan, Department of Mathematics, University of Florida, Gainesville, FL 32611, USA.